Journal of Alloys and Compounds 477 (2009) 182–187

Contents lists available at ScienceDirect

Journal of Alloys and Compounds

journal homepage: www.elsevier.com/locate/jallcom

Large hydrogen capacity in hydrides R_2Ni_2In–H (R = La, Ce, Pr, Nd) with new structure type

M. Dzevenko[a,b], K. Miliyanchuk[a,b], Ya. Filinchuk[c], O. Stelmakhovych[b], L. Akselrud[a], L. Havela[b,*], Ya. Kalychak[a]

[a] Faculty of Chemistry, Ivan Franko National University of Lviv, Kyryla i Mefodiya 6, 79005 Lviv, Ukraine
[b] Department of Condensed Matter Physics, Charles University, Ke Karlovu 5, 121 16 Prague 2, Czech Republic
[c] SNBL at ESRF, BP 220 38043 Grenoble, France

ARTICLE INFO

Article history:
Received 22 July 2008
Received in revised form 9 October 2008
Accepted 14 October 2008
Available online 3 December 2008

PACS:
61.66.Dk
75.50.Ee

Keywords:
Rare earth alloys and compounds
Hydrogen absorbing materials
X-ray diffraction
Magnetic measurements

ABSTRACT

Several new hydrides with the composition $R_2Ni_2InH_x$ (R = La, Ce, Pr, Nd; $x \approx 4.5$–5.0) were synthesized. They are based on the R_2Ni_2In compounds crystallizing in the Mo_2FeB_2 structure type. So as to accommodate high amount of H atoms (x can theoretically reach the value of 6), the structure changes to orthorhombic, space group *Pbam*, while the unit-cell volume increases by 10–20%. Nd_2Ni_2In was found antiferromagnetic, with a first-order magnetic phase transition at $T_N = 8$ K. Applied magnetic field $\mu_0 H < 0.3$ T induces ferromagnetism. T_N of $Nd_2Ni_2InH_{4.5}$, which is a more regular antiferromagnet, is reduced to 5 K.

1. Introduction

R_2T_2In compounds belong to a large family of rare-earth (and also actinide) based compounds, which crystallize with the Mo_2FeB_2 structure type (space group *P*4/*mbm*) (for overview see Refs. [1,2] and references therein). Their structure type is characterized by bilayers along the shortest lattice parameter *c*, and consists of trigonal (type AlB_2) and tetragonal (type CsCl) prisms. Such materials have been studied from the point of view of 4f magnetism for R from the group of regular rare earths; anomalous rare earths (Ce, Yb) were studied in terms of valence fluctuations of the 4f elements (as Ce_2Ni_2In and Ce_2Rh_2In [3,4]). Ce_2Cu_2In is characterized by antiferromagnetic order below 5.5 K, whereas for its hydride $Ce_2Cu_2InH_{2.8}$ the fingerprint of magnetic order was lost [5]. The compounds R_2Cu_2In (R = Gd–Tm) exibit ferromagnetic behaviour with $T_C \approx 90$ K or lower [6]. Finally, those including light actinides (mostly U) were investigated with the aim to better understand the peculiarities of the 5f band magnetism, for which the varying type of the nearest-neighbour spacing of the magnetic atoms within one structure type provides a unique opportunity. Another degree of freedom of the Mo_2FeB_2 structure type is offered by the possibility of interstitial doping by hydrogen, which was demonstrated for U_2T_2Sn and U_2T_2In compounds, modifying considerably their magnetic properties [7,8].

In this paper we describe the results of the investigation of hydrogen absorption properties of R_2Ni_2In (R = La, Ce, Pr, Nd) compounds (following a preliminary report in Ref. [9]). We introduce basic properties of this new class of materials, including details of crystal structure of the hydrides.

2. Experimental

R_2T_2In compounds were prepared by arc melting of pure elements (the nominal purity R—99.8 wt.% R, Ni—99.99 wt.% Ni, and In—99.99 wt.% In) under Ar atmosphere. The buttons were melted two times to ensure homogeneity. The total mass of each alloy was about 1 g. The mass losses during melting did not exceed 1%.

The alloys were subsequently crushed in sub-millimeter pieces and heated to $T = 473$ K in vacuum (better than 1×10^{-6} mbar) so as to remove adsorbed impurities. After introducing hydrogen gas, samples started to absorb hydrogen readily. The hydrogenation was carried out at the room temperature and hydrogen pressure 500 mbar. The hydrogen absorption was monitored by the pressure drop in the system. The amount of hydrogen absorbed was recalibrated to ambient temperature, yielding the stoichiometry of the compounds used below.

* Corresponding author. Tel.: +420 221911351.
E-mail address: havela@mag.mff.cuni.cz (L. Havela).

0925-8388/$ – see front matter © 2008 Elsevier B.V. All rights reserved.
doi:10.1016/j.jallcom.2008.10.042

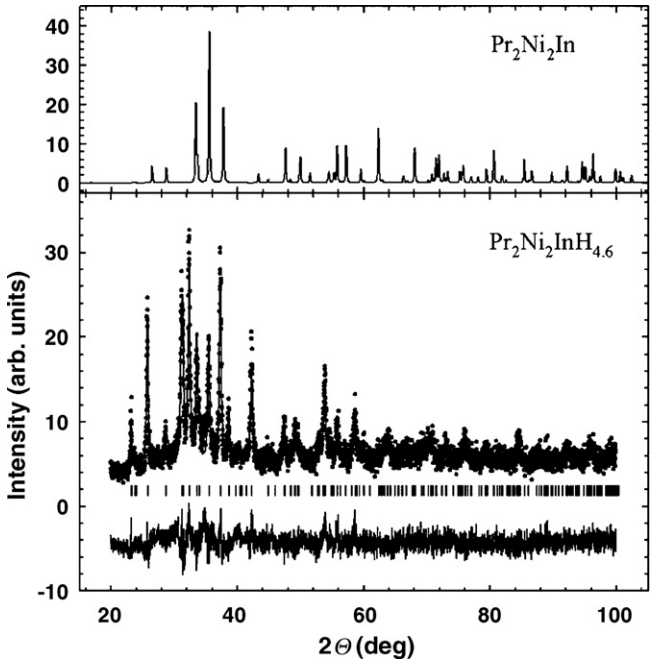

Fig. 1. Theoretical X-ray diffraction pattern of Pr_2Ni_2In (upper panel); observed (♦), calculated (–), and difference X-ray diffraction pattern of $Pr_2Ni_2InH_{4.6}$ hydride.

The crystal structure was investigated by means of X-ray powder diffraction, using the HZG-4a (Cu Kα-radiation) or Seifert XRD7 (Cu $K\alpha_1$-radiation, graphite monochromator) diffractometers. The programs Fullprof [10] and CSD [11] were used for the data analysis.

Pr_2Ni_2In–H was studied by 2D (MAR345 IP) synchrotron powder diffraction at the Swiss-Norwegian Beam Lines (λ = 0.0808136 nm) at ESRF (Grenoble, France). Quantum Design PPMS equipment was used for the magnetic and heat capacity studies of Nd_2Ni_2In and its hydride $Nd_2Ni_2InH_{4.5}$ in the temperature range 2–300 K and magnetic fields up to 9 T (magnetization) or 12 T (heat capacity). In the magnetization study, the grains of the samples were fixed in random orientation by acetone-soluble glue, which prevents any rotation of individual grains under the influence of a magnetic field. The heat capacity was measured on a bulk piece for Nd_2Ni_2In and on a pellet produced by pressing the powder in a die with WC piston faces in the case of the hydride.

3. Results and discussion

3.1. Structure studies

The hydrogenation process as described above led for all R_2Ni_2In (R = La, Ce, Pr, Nd) compounds to a hydrogen absorption corresponding to approximately 4.5 H atoms per formula unit and to structure modifications. The first inspection of X-ray diffraction patterns indicated that the hydrides are isostructural and their structure is different than that of the initial compounds (see Fig. 1 showing the patterns of Pr_2Ni_2In and $Pr_2Ni_2InH_{4.6}$). The finding

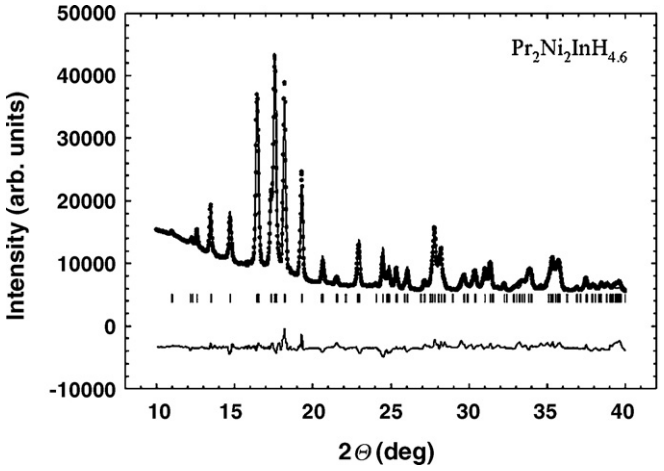

Fig. 2. Observed (♦), calculated (–), and difference synchrotron diffraction pattern of $Pr_2Ni_2InH_{4.6}$ hydride at room temperature (λ = 0.0808136 nm).

that we indeed deal with single-phase hydrides was corroborated by the fact that the temperature-induced H desorption, which is completed below about $T = 1273$ K, recovers the original crystal structure. In case the hydrogenation was suspended before the full absorption was achieved, a mixture of the initial compound and the hydride was observed in the X-ray diffraction pattern. This suggests that the hydrides obtained are in fact β-hydrides, separated from the initial structure by a two-phase region.

A more detailed X-ray diffraction analysis shows that the formation of hydrides leads to an anisotropic expansion of the unit cells in the [1 0 0] direction, with a small compression in the [0 1 0] and [0 0 1] directions. The unit cell volume expansion is quite large, considerably exceeding 10% (see Table 1). As a result of the anisotropic expansion, the symmetry changes from tetragonal to orthorhombic, adopting with the space group *Pbam*. Crystal structure data and details of structure refinement are listed in Table 2. A certain exception is represented by Ce_2Ni_2In, which tends to decompose in the course of the hydrogenation process, forming besides the quaternary hydride $Ce_2Ni_2InH_{4.8}$ also two spurious phases Ce_7Ni_3 (space group $P6_3mc$) and Ce_2Ni_7 (space group $P6_3/mmc$).

The synchrotron-radiation investigation of $Pr_2Ni_2InH_{4.6}$ hydride was performed on the sample sealed into a glass capillary (0.2 mm diameter) using the wavelength λ = 0.808136 Å (Fig. 2). The data obtained confirmed the results of the conventional X-ray diffraction. The lattice parameters obtained are: $a = 0.84366(7)$, $b = 0.75524(6)$, $c = 0.38120(3)$ nm, $V = 0.24289(6)$ nm^3 ($R_I = 11.0\%$, $R_P = 16.4\%$). The atomic coordinates and thermal parameters are following: Pr 4*h* *x y* 1/2 ($x = 0.6807(5)$, $y = 0.1700(6)$); Ni 4*g* *x y* 0 ($x = 0.0983(9)$, $y = 0.6468(12)$); In 2*a* 0 0 0; $B_{iso} = 0.0078(7)$ nm^2 for all atoms. The lattice parameters and atomic coordinates are quite different for the samples measured with Cu Kα-radiation and syn-

Table 1
Crystallographic data of R_2Ni_2In (R = La, Ce, Pr, Nd) compounds and their hydrides.

Compound	Space group	*a* (nm)	*b* (nm)	*c* (nm)	$\Delta V/V_0$ (%)
La_2Ni_2In	*P*4/*mbm*	0.7636(2)	–	0.3906(2)	–
$La_2Ni_2InH_{5.0}$	*Pbam*	0.9079(4)	0.7608(4)	0.3782(3)	14.7
Ce_2Ni_2In	*P*4/*mbm*	0.7527(2)	–	0.3722(1)	–
$Ce_2Ni_2InH_{4.8}$	*Pbam*	0.8995(4)	0.7549(4)	0.3720(2)	19.5
Pr_2Ni_2In	*P*4/*mbm*	0.7525(2)	–	0.3819(1)	–
$Pr_2Ni_2InH_{4.6}$	*Pbam*	0.8930(4)	0.7511(3)	0.3712(2)	14.8
$Pr_2Ni_2InH_{4.6-x}$[a]	*Pbam*[a]	0.84366(7)[a]	0.75524(6)[a]	0.38120(3)[a]	12.5[a]
Nd_2Ni_2In	*P*4/*mbm*	0.7506(2)	–	0.3789(1)	–
$Nd_2Ni_2InH_{4.5}$	*Pbam*	0.8448(5)	0.7505(5)	0.3888(3)	15.5

[a] Synchrotron data.

Table 2
Crystal data and structure refinements for $R_2Ni_2InH_x$ compounds.

Empirical formula	$La_2Ni_2InH_{5.0}$	$Ce_2Ni_2InH_{4.8}$	$Pr_2Ni_2InH_{4.6}$	$Nd_2Ni_2InH_{4.5}$
Molar mass (g/mol)	515.06	517.28	518.66	525.12
Equipment	Seifert XRD7	HZG-4a	Seifert XRD7	Seifert XRD7
Wavelength	Cu Kα	Cu Kα	Cu Kα	Cu Kα
2θ range for data collection	20.0–100.0°	15.0–145.0°	20.0–100.0°	15.0–120.0°
Step size in 2θ	0.02°	0.05°	0.02°	0.04°
Space group	*Pbam*	*Pbam*	*Pbam*	*Pbam*
Atoms coordination				
R 4*h* (*x y* 1/2)	*x* = 0.686(2)	*x* = 0.683(1)	*x* = 0.685(1)	*x* = 0.682(3)
	y = 0.160(2)	*y* = 0.158(1)	*y* = 0.163(1)	*y* = 0.165(3)
Ni 4*g* (*x y* 0)	*x* = 0.093(3)	*x* = 0.095(3)	*x* = 0.096(3)	*x* = 0.100(5)
	y = 0.671(4)	*y* = 0.663(5)	*y* = 0.660(4)	*y* = 0.653(6)
In 2*a* (0 0 0)				
R_f (%)	4.7	6.4	8.0	12.0
R_{Bragg} (%)	9.6	12.1	11.8	13.3

chrotron radiation, what might be a consequence of the hydride instability in time or at the crushing or other treatment. The comparison of lattice parameters indicates that the hydrogen content can be significantly lower in the sample at the synchrotron experiment. Therefore we denote this sample as $Pr_2Ni_2InH_{4.6-x}$.

The coordination polyhedra for Pr atoms in the initial structure (Mo_2FeB_2-structure type) are pentagonal prism with additional atoms (coordination number 17), for Ni atoms—trigonal prism with additional atoms (9), and for In atoms—tetrahexahedron (14). In the hydride, the structures of the coordination polyhedra change due to increase of the lattice parameter *a*. The coordination number for Pr atoms is changed to 15, and for Ni atoms—to 8. The coordination number of In atoms is 14. The projection of $Pr_2Ni_2InH_{4.6}$ on *XY* plane is shown in Fig. 3. The interatomic distances are listed in Table 3.

The orthorhombic deformation of the crystal structure, which occurs during the hydride formation (*P4*/*mbm* → *Pbam*), leads to a small deformation of the AlB_2- and CsCl-type fragments. Consequently, it deforms the existing interstitials in the structure. The structure can be considered as a packing of trigonal-bipyramid R_3Ni_2, tetrahedral R_2In_2 and octahedral R_4NiIn interstitials (Fig. 4), which surround the interstitials described by Wyckoff position 4*h* for R_3Ni_2 and R_2In_2 and 4*g* for R_4NiIn (Table 4). The analysis of the data presented in Table 4 shows that some interstitials, i.e. H21 and H32 do not satisfy geometrical and size criteria. Therefore, the favorable positions for hydrogen atoms are H1, H22, and H31, and they allow accommodating up to 6 hydrogen atoms per formula unit.

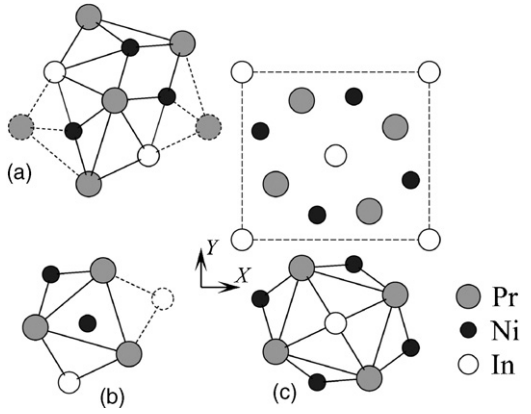

Fig. 3. Projection of the structure of the metallic matrix for $Pr_2Ni_2InH_{4.6}$ hydride onto the *XY* plane and the coordination polyhedra of atoms: *a*-Pr, *b*-Ni, *c*-In. Atoms and bonds, which belong to the coordination polyhedra of the initial structure, are marked by dotted lines.

Table 3
Interatomic distances in $Pr_2Ni_2InH_{4.6-x}$ from synchrotron X-ray powder diffraction experiment all distances within the first coordination spheres are listed.

Atom		δ (Å)	CN
Pr	2 Ni	3.004(7)	15
	2 Ni	3.034(7)	
	2 Ni	3.137(8)	
	2 In	3.488(4)	
	2 In	3.541(4)	
	2 Pr	3.812(0)	
	2 Pr	3.953(6)	
	2 Pr	3.987(6)	
Ni	1 Ni	2.769(12)	8
	1 In	2.794(9)	
	2 Pr	3.004(7)	
	2 Pr	3.034(7)	
	2 Pr	3.137(8)	
In	2 Ni	2.794(9)	14
	4 Pr	3.488(4)	
	4 Pr	3.541(4)	
	2 Ni	3.566(8)	
	2 In	3.812(0)	

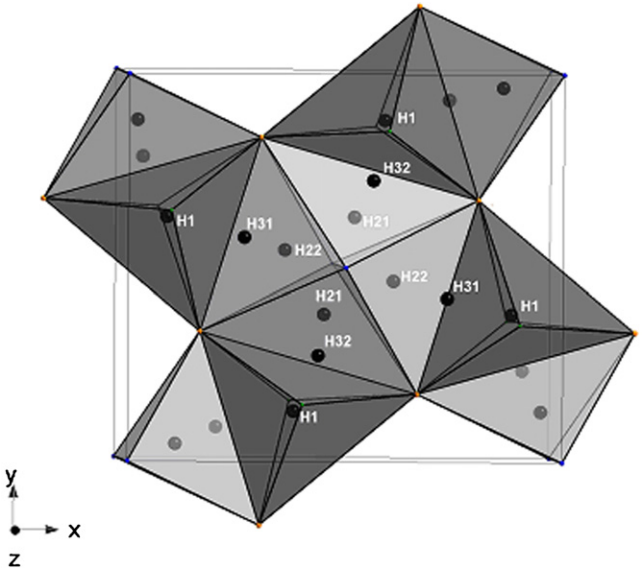

Fig. 4. Three-dimensional arrangements of interstitials in the $Pr_2Ni_2InH_{4.6}$ structure.

Table 4
Crystallographic parameters of the existing interstitials for the structure of $Pr_2Ni_2InH_{4.6}$ (Wyckoff position and atomic coordinates of the possible hydrogen sites *x*, *y*, *z*, and calculated interatomic distances to the metal atoms and between themselves).

Interstitial	Wyckoff position	*x*	*y*	*z*	δ_{H-Pr} (nm)	δ_{H-Ni} (nm)	δ_{H-In} (nm)	
R_3Ni_2	H1	4*h*	0.40	0.12	0.5	0.23	0.19	0.35
R_2In_2	H21	4*h*	0.46	0.38	0.5	0.24	0.26	0.21
	H22	4*h*	0.38	0.46	0.5	0.22	0.31	0.22
R_4NiIn	H31	4*g*	0.23	0.08	0	0.27	0.15	0.20
	H32	4*g*	0.44	0.27	0	0.29	0.10	0.18

Calculated distances

δ_{H-H} (nm)	H1	H21	H22	H31	H32
H1	0.26	0.20	0.24	0.24	0.22
H21		0.20	0.15	0.30	0.20
H22			0.22	0.21	0.28
H31				0.38	0.23
H32					0.36

3.2. Magnetic properties and heat capacity

Nd_2Ni_2In has rather unusual magnetic properties. The temperature dependencies of magnetic susceptibility measured in high fields (3 and 6 T) seem to indicate a ferromagnetic order below $T \approx 10$ K (see Fig. 5). On the other hand, the Curie–Weiss behavior in the paramagnetic range, which yields a negative paramagnetic Curie temperature $\theta_p = -4.5$ K points to antiferromagnetic interactions. The calculated effective moment $\mu_{eff} = 3.65\mu_B$/Nd is close to the theoretical value for $4f^3$ configuration ($3.62\mu_B$). The susceptibility measurement in low magnetic fields shows a pronounced increase (faster than the extrapolated Curie–Weiss fit) of susceptibility at $T = 8$ K, followed by a flat part and eventually a downturn on the low temperature side. The magnetization curve at $T = 2$ K (Fig. 6) resembles that of ferromagnet, it exhibits a certain hysteresis in the low-field range (below 1 T), but there is practically no remanent magnetization. The spontaneous magnetization obtained by extrapolation from the high-field state corresponds to $2.5\mu_B$ per formula unit (i.e. $1.25\mu_B$/Nd atom). The pronounced high-field slope tends to saturation at $\approx 3.9\mu_B$ per formula unit. The saturated magnetization per Nd atom, $\mu_{sat} \approx 2.0\mu_B$/Nd, is still considerably lower that the magnetization of free Nd ion ($3.27\mu_B$), which can be understood as due to crystal-field effects or possible incomplete collinearity in available magnetic fields.

A deeper insight is provided by heat capacity, $C(T)$, measurement. A very pronounced anomaly at $T = 8$ K related to the magnetic phase transition (Fig. 7) is clearly of a first-order type, being dissimilar to a standard λ-type transition, pertinent to second-order phase transitions. Although magnetic entropy can be traced out even far below the ordering temperature as the part of C/T which gets suppressed by magnetic field, it turns up abruptly above $T = 7.5$ K reaching a climax at $T = 8.0$ K. The sharp character withstands magnetic fields up to 0.1 T. From the field $\mu_0 H = 0.3$ T, it starts to broaden and shifts gradually towards higher temperatures, as usual in a ferromagnet. It means that the first-order magnetic phase tran-

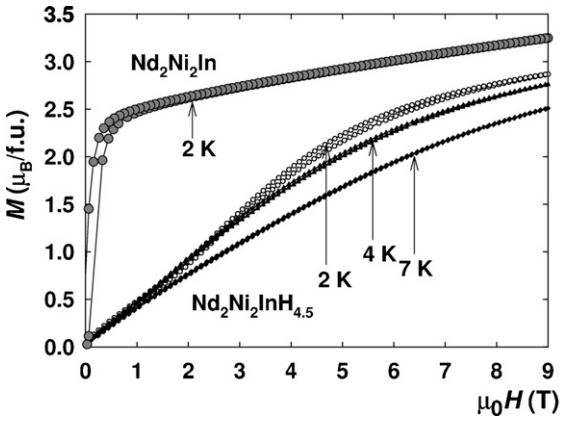

Fig. 6. Magnetic field dependence of the magnetization for Nd_2Ni_2In and $Nd_2Ni_2InH_{4.5}$ at various temperatures.

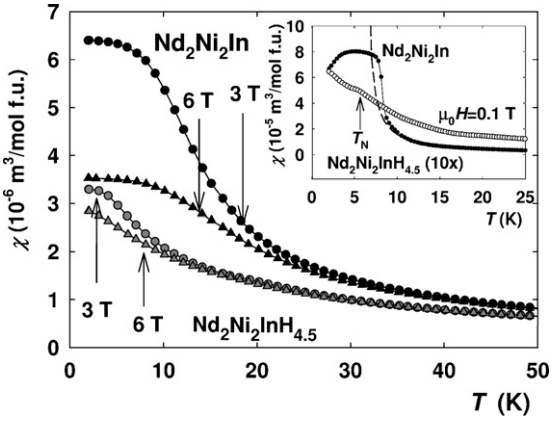

Fig. 5. Temperature dependence of the magnetic susceptibility for Nd_2Ni_2In and $Nd_2Ni_2InH_{4.5}$ measured in fields of 3 and 6 T. The inset shows the detail in weak magnetic field (0.1 T).

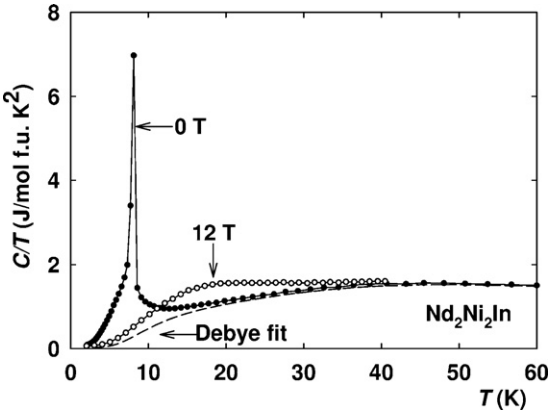

Fig. 7. Temperature dependence of the specific heat (in the C/T vs. T representation) for Nd_2Ni_2In. The lattice specific heat approximated by the Debye model with $\theta_D = 200$ K is shown by the dashed line for comparison.

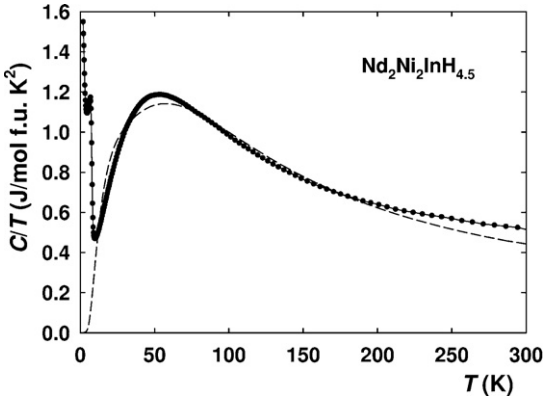

Fig. 8. Temperature dependence of the specific heat (in the C/T vs. T representation) for $Nd_2Ni_2InH_{4.5}$. The dashed line shows the dependence for the Debye model with $\theta_D = 200$ K.

sition changes into the standard second-order type only in fields exceeding 0.1 T.

Such peculiar behaviour can be for example a consequence of a frustration of magnetic interactions due to symmetry constraints of the crystal lattice. It is interesting to realize that collinear antiferromagnetism is allowed by the group symmetry only if magnetic moments of R atoms are along the *c*-axis. If magnetic anisotropy requires moments in the basal plane, the moments cannot be collinear. Instead one of several types of orthogonal arrangement has to be adopted [12]. In such scheme, we may speculate that a lattice distortion appearing presumably at T_N modifies the symmetry constraints present in the high-symmetry paramagnetic phase, allowing for a new type of antiferromagnetic phase.

The character of magnetic ordering changes in $Nd_2Ni_2InH_{4.5}$. The paramagnetic behaviour is similar to the parent intermetallic, but the θ_P value, −9.7 K, is more negative, and the effective moment of $3.55\mu_B$ per one Nd atom somewhat smaller than in the non-hydrogenated compound. The antiferromagnetic order can be associated with the kink in magnetic susceptibility at $T = 5$ K (see inset of Fig. 5). Below this temperature, a weakly metamagnetic behaviour develops, with an inflection around $\mu_0 H = 4$ T (Fig. 6). The saturated magnetization remains somewhat lower than for Nd_2Ni_2In. Although the hydride has undoubtedly antiferromagnetic ground state, the susceptibility does not form a well-defined cusp. As in similar cases, the small-grain form of the hydride, emphasize the importance of grain boundaries. The incomplete

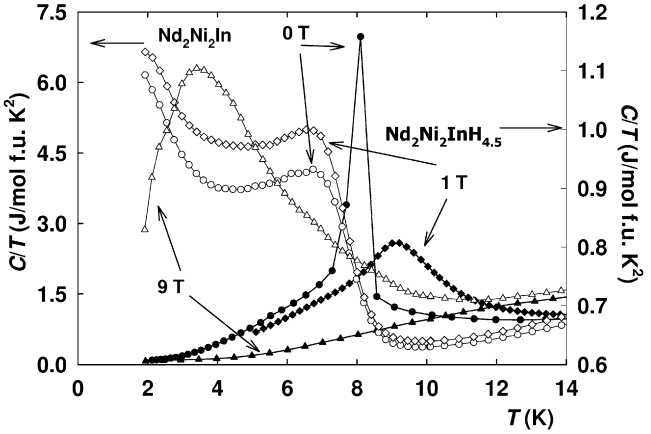

Fig. 9. Temperature dependence of the specific heat for Nd_2Ni_2In and $Nd_2Ni_2InH_{4.5}$ obtained in various magnetic fields (filled symbols—Nd_2Ni_2In, blank—$Nd_2Ni_2InH_{4.5}$).

mutual cancellation of sublattice magnetizations at grain boundaries induces in such case a weak parasitic ferromagnetic signal. Also defects due to incomplete occupancy of H sites can contribute to this effect.

The temperature dependence of the specific heat for $Nd_2Ni_2InH_{4.5}$ shows pronounced magnetic anomaly at $T = 7$ K, that is slightly higher in comparison with magnetization data. The low-temperature upturn below 5 K (Figs. 8 and 9) is suppressed upon applying the magnetic field of 9 T.

4. Concluding remarks

It is interesting to compare the evolution of magnetic properties with hydrogenation of the R_2Ni_2In group with other analogous rare-earth-based ternary compounds. It seems that there is, at least for regular rare earths, a net tendency of weakening magnetic interactions [13]. The reason can be found in the fact, that H doping into strongly electropositive rare earths represents an anionic doping, with H binding extra conduction electrons, which are therefore removed from the vicinity of the Fermi level. This has to weaken the RKKY exchange interaction, depending on the polarization of conduction electron states. For Nd_2Ni_2In and its hydride, the drop of the reduction of ordering temperatures from 8 to 5 K follows the same tendency, but is not that large as e.g. in RNiAl. Studies of magnetic properties of other R_2Ni_2In compounds and their hydrides should reveal if for example a frustrated order can be in fact the reason for anomalously low ordering temperatures in Nd_2Ni_2In.

It is also interesting to compare in Nd_2Ni_2In with in U_2Ni_2In, as U has the electronic configuration close to f^3. The hydrogen concentration for the U-based 221 compounds known so far does not exceed 2 H atoms/f.u., the volume expansion is lower than 10%, and the tetragonal symmetry is preserved [14]. While skip U_2Ni_2In orders antiferromagnetically at $T_N = 15$ K, $U_2Ni_2InH_{1.9}$, which preserves the tetragonal structure, orders at $T_N = 60$ K [14]. The qualitative difference is that unlike the localized 4f states in Nd, the U 5f states form a band of strongly correlated states at the Fermi level. The related density of states can therefore react to the lattice expansion (band narrowing) by an increase. This leads to more emphasized magnetism in the hydride.

Acknowledgments

This work was part of the research plan MSM 0021620834 financed by the Ministry of Education of the Czech Republic. It was supported by the Grant Agency of the Czech republic under the grant no. 202/07/0418. The authors would like to express their gratitude to RNDr. Stanislav Daniš for the assistance with the X-ray diffraction experiment and SNBL for in-house beamtime allocation.

References

[1] Ya.M. Kalychak, V.I. Zaremba, R. Pöttgen, M. Lukachuk, R.-D. Hoffman, in: K.A. Gschneidner Jr., J.-C. Bünzli, V. Pecharsky (Eds.), Handbook on the Physics and Chemistry of Rare Earths, vol. 34, Elsevier, Amsterdam, 2004, pp. 1–133.
[2] Ya.M. Kalychak, V.I. Zaremba, V.M. Baranyak, P.Yu. Zavaliy, V.A. Bruskov, L.V. Sysa, O.V. Dmytrakh Izv, AN SSSR Inorg. Mater. 26 (1990) 94 (in Russian).
[3] M. Giovannini, E. Bauer, H. Michor, G. Hilscher, A. Galatanu, A. Saccone, P. Rogl, Intermetallics 9 (2001) 481.
[4] D. Kaczorowski, P. Rogl, K. Hiebl, Phys. Rev. B 54 (1996) 9891.
[5] K. Miliyanchuk, A.V. Kolomiets, Ya.V. Galadzhun, L. Havela, I.I. Bulyk, A.M. Trostianchyn, Ya.M. Kalychak, Chem. Met. Alloys 1 (2008) 46.
[6] I.R. Fisher, Z. Islam, P.C. Canfield, J. Magn. Magn. Mater. 202 (1999) 1.
[7] K. Miliyanchuk, L. Havela, A.V. Kolomiets, A.V. Andreev, Physica B 359–361 (2005) 1042.
[8] K. Miliyanchuk, L. Havela, L.C.J. Pereira, A.P. Gonçalves, K. Prokeš, J. Magn. Magn. Mater. 310 (2007) 945.

[9] M. Dzevenko, K. Miliyanchuk, Ya. Filinchuk, L. Havela, Ya. Kalychak, Proceedings of the Collected Abstracts of the XIth Scientific Conference "Lviv Chemical Readings", Lviv (Ukraine), May, 2007, p. H31 in Ukrainian.
[10] J. Rodriguez-Carvajal, FULLPROF, version 2.80, July 2004, ILL.
[11] L.G. Akselrud, Yu.N. Gryn', P.Yu. Zavalij, V.K. Pecharsky, V.S. Fundamensky, Collected Abstracts of the 12th European Crystallographic Meet., vol. 3, Moscow, August, 1989, Izv. Akad. Nauk. SSSR, p.155.
[12] F. Bourée, B. Chevalier, L. Fournès, F. Mirambert, T. Roisnel, V.H. Tran, Z. Zolnierek, J. Magn. Magn. Mater. 138 (1994) 307.
[13] A. Kolomiets, L. Havela, A.V. Andreev, V. Sechovsky, V.A. Yartys, J. Alloys Compd. 262–263 (1997) 206.
[14] K. Miliyanchuk, L. Havela, A.V. Kolomiets, S. Daniš, L.C.J. Pereira, A.P. Gonçalves, Physica B 378–380 (2006) 983.